



Contents lists available at ScienceDirect

Arabian Journal of Chemistry

journal homepage: www.ksu.edu.sa

Original article

pH-responsive release of ciprofloxacin hydrochloride from micro-, nano-, and functionalized nanocellulose

Hridoy Roy^a, Khalide Hasan Parvej^b, Mohammad Mozammel Hosen^{b,c}, Md. Shahinoor Islam^a, Shakhawat H. Firoz^{b,*}^a Department of Chemical Engineering, Bangladesh University of Engineering and Technology, Dhaka 1000, Bangladesh^b Department of Chemistry, Bangladesh University of Engineering and Technology, Dhaka 1000, Bangladesh^c Chemistry Division, Atomic Energy Centre, Bangladesh Atomic Energy Commission, Dhaka-1000, Bangladesh

ARTICLE INFO

Keywords:

Selective functionalization
 Nanocellulose
 pH responsiveness
 Kinetics
 Di-aldehyde nanocellulose

ABSTRACT

This research evaluated pH-responsive release characteristics for the drug (ciprofloxacin hydrochloride) from micro-, nano-, and functionalized cellulose forms. Nanocrystalline cellulose (NCC) was prepared from microcrystalline cellulose (MCC) by sulfuric acid hydrolysis. The aldehyde (–CHO) groups were introduced at the carbon-2 (C-2) and carbon-3 (C-3) positions of glucose moiety of the cellulose network by selective oxidation to form di-aldehyde nanocellulose (DANC). The conversion was validated by chemical, spectroscopic, morphological, and crystallographic analysis. Drug binding capacity (mg/g) of DANC was higher (200.8 mg/g) compared to NCC (138.3 mg/g) and MCC (120.2 mg/g), respectively. The increase in pH from 2.5 to 8.5 enhanced drug release for all the excipients. At pH 2.5, slow release of the drugs was observed. In 6 h, DANC released 44.7 % of the loaded drug at pH 2.5. However, drug release reached equilibrium (84.8 % of loaded drug) within 10 min at pH 8.5. The release kinetics at acidic pH were validated using zero-order, first-order, Higuchi, and Korsmeyer-Peppas kinetics models. Higuchi and Korsmeyer–Peppas' kinetic models interpreted drug release phenomena with a good fit. This implies that diffusion, dissolution, swelling, and slight erosion contribute to drug release. The results suggest that selective functionalization can be applied to cellulose for its potential applications in pH-responsive drug delivery, and therefore, the functionalized cellulose deserves immediate attention.

1. Introduction

Continuous advancement in the medical and pharmaceutical sectors has accelerated the research on the discovery and trial of stimuli-responsive controlled drug delivery systems (Gao et al., 2023). In the last few decades, controlled drug delivery has received enormous attention due to its advanced and potential applications, e.g., maintaining drug levels at a desired range, minimizing dosing frequency, preventing over or under-dosing, and nullifying side-effects (Mura et al., 2022, Pooresmaeil et al., 2023). Natural polymers, e.g., starch, cellulose, chitosan, alginates, etc. are widely used by the pharmaceutical industries to act as drug excipients (Ahmad et al., 2020, Pal and Raj, 2023). These excipients bind active ingredients and release these ingredients upon dissolving or swelling or other methods. The most abundant natural polymer, cellulose, and its derivatives have excellent compaction, biodegradable, and binding properties, which help these

polymers to blend with active ingredients and form compact matrices suitable for oral administration of drugs (Seddiqi et al., 2021). There are different forms of raw cellulose used in drug delivery systems, such as microcrystalline cellulose (MCC) (O'Connor and Schwartz, 1993), and nanocrystalline cellulose (NCC) (Pachua, 2017). However, functionalized cellulose, e.g., ethyl cellulose (Crowley et al., 2004), carboxymethyl cellulose, cellulose esters (Edgar, 2007) are extensively used as oral, topical, and injectable excipients in controlled drug-delivery systems due to their excellent hydrophobicity, biocompatibility, porosity, and swelling characteristics. Therefore, considerable research is ongoing on different types of cellulosic materials in advanced excipient system design to solve their irreversible behavior, lack of drug binding capacity, inefficient stimuli responses, etc. However, the functionalization of raw cellulose is costly and induces cytotoxic properties in the structure. Therefore, altering cellulose structure with other materials sometimes becomes unfeasible for drug delivery applications. MCC, a microcrystal

* Corresponding author.

E-mail addresses: hridoyroy@che.buet.ac.bd (H. Roy), shfiroz@chem.buet.ac.bd (S.H. Firoz).<https://doi.org/10.1016/j.arabjc.2024.105763>

Received 22 February 2024; Accepted 25 March 2024

Available online 27 March 2024

1878-5352/© 2024 The Author(s). Published by Elsevier B.V. on behalf of King Saud University. This is an open access article under the CC BY-NC-ND license (<http://creativecommons.org/licenses/by-nc-nd/4.0/>).

form of cellulose, is utilized in the drug delivery field (Anis Yohana et al., 2019). Partial negative surface charge ($-OH$ groups in 2,3,6 position) of MCC binds with the drug molecules. However, MCC has a relatively small surface area compared to its large insoluble mass, which reduces its efficiency in binding a good amount of drug particles. However, NCC, a nanoform of cellulose, offers several advantages over MCC in being used as an excipient. Size reduction enhances its surface area to a greater extent, and more exposed hydroxyl ($-OH$) groups can attach a large amount of drug particles to its surface (Alavi, 2019). In addition, the nano-size of particles enhances their sorption and release nature significantly (Gharbani, 2017; Gharbani et al., 2022). This can be utilized in high payloads of drugs and controlled/optimum dosing (Jackson et al., 2011, Gharbani et al., 2015). Moreover, cellulose nanofibers are being utilized in drug delivery with Pickering emulsions as a stabilizer (Li and Yu, 2023a). Zhuo Li and Dehai Yu (2023) reported the formulation and characterization of pH-responsive Pickering emulsions for controlled delivery (Li and Yu, 2023b). In addition, Zhuo Li et al., (2024) reported on enhancing emulsification and drug delivery mechanism (Li et al., 2024). However, there is very little research on the use of MCC and NCC for controlled drug delivery due to their reluctance to the stimuli-response. Thus, chemical modification of the existing hydroxyl groups in NCC can increase the process-ability, efficiency, and applicability of NCC as an excellent drug delivery excipient. Common practices in this regard include esterification (Wang et al., 2018) and etherification (Heinze et al., 2018) of the available hydroxyl groups. Other than these, oxidation is another important approach for the chemical functionalization of NCC (Motiur Rahman et al., 2021). However, most of the oxidation reactions are not selective and effective. Selective oxidation is very useful to bring the desired change in a structure; e.g., by cleaving the C-2 and C-3 bond via periodate is one of the modifications of the cellulose chain leading to the introduction of aldehyde functional groups to form di-aldehyde nanocrystalline cellulose (DANC) (Siller et al., 2015, Mou et al., 2017). With the difference in form, structure, chemical functionalities, and surface texture, DANC can be distinguishable from MCC and NCC and requires systematic research to find its suitability as an excipient in drug delivery. The DANC can be an excellent drug carrier that can serve pH-responsive controlled drug release due to its selective oxygenated functional groups. However, very few researchers explored the vast prospects of cellulose derivatives in this regard and there is no research available that studied drug release characteristics of the DANC. It is expected that the functionalization of surfaces can interact with drugs selectively, and this functionalization can be designed according to the need to control the release of a particular target drug. Hence, in this research, we have made an effort to synthesize DANC by the selective oxidation of NCC and studied the pH response of the release of a model drug (ciprofloxacin hydrochloride) on DANC along with NCC and MCC in a simulated gastrointestinal environment. Moreover, to understand the in-depth of the release, kinetics of the release has been analyzed critically. The study has led to some interesting and promising conclusions regarding the application of synthesized materials.

2. Materials and methods

2.1. Material and chemicals

MCC (HPLC grade, Sigma Aldrich, Germany), 98 % (w/w) sulfuric acid (Merck, Germany), sodium periodate (Sigma Aldrich, Germany), ethylene glycol (Sigma Aldrich, Germany), and ciprofloxacin hydrochloride (Merck, Germany). To modify cellulose and prepare drug solutions, deionized (DI) water was used.

2.2. Synthesis of DANC from MCC via NCC

Initially, NCC was synthesized from MCC following a standard protocol reported by Amzad et al., (2020) (Hossain et al., 2020). Initially, 5 g of as received MCC was taken in a round bottom flask (500 mL) and

mixed with 100 mL 63.5 % (w/w) sulfuric acid (H_2SO_4) to maintain 1:20 (MCC: H_2SO_4) ratio. The mixture was then placed in an oil bath (dimensions: 130 cm (diameter) x 60 cm (height), temperature range 0–260 °C) at 60 °C and continuously stirred at 100 rpm (G-force: 1 RCF) for 1.5 h for acid hydrolysis. The hydrolysis reaction was then terminated by a tenfold dilution of the suspension with DI water. The diluted suspension was subjected to ultra-sonication at 80 kHz frequency. After sonication, the suspension was settled for 12 h, when two distinctive layers were formed. The top layer was decanted off, and washing with DI was continued until a milky white cloudy suspension (dispersion) was obtained. The cloudy dispersion of NCC was centrifuged repeatedly at 6000 rpm (G-force: 1210 RCF) to separate water-soluble particles and excess reagents until filtrate pH approached approximately 4. Further, NCC suspension was dialyzed (in a dialysis tube) against DI water to obtain a steady pH of 4 for the filtrate. The NCC was then stored in a refrigerator at 5 ± 1 °C for further characterization and DANC formation.

For C-2 and C-3 oxidation of synthesized NCC, 1000 mL of 2 % (w/v) NCC suspension was taken in a round bottom flask (2 L), and 26.76 g sodium periodate ($NaIO_4$) was poured into the NCC suspension to be mixed in a magnetic stirrer. The flask was placed in an oil bath (dimensions: 130 cm (diameter) x 60 cm height), temperature range 0–260 °C) at 48 °C. The whole oil bath-flask set-up was covered with aluminum foil to resist light penetration. The absence of light and temperature (48 °C) was maintained precisely for the desired oxidation of NCC. To terminate the reaction, after 20 h of stirring, excess ethylene glycol ($C_2H_6O_2$) was poured into the reaction mixture. DI water was then used to wash the product. The washed product was then repeatedly centrifuged at 4000 rpm (G-force: 538 RCF). Further dialysis was performed to wash foreign particles and ions on di-aldehyde nanocellulose (DANC). The whitish cloudy suspension of DANC was stored in a refrigerator at 5 ± 1 °C for characterizations and experiments.

2.3. Characterizations

The formation of DANC from NCC was confirmed by chemical, spectroscopic, morphological, and crystallographic analysis. The chemical characterization was carried out through 2, 4-dinitrophenylhydrazine (2,4-DNPH) test. For spectroscopic analysis, Fourier-transform infrared spectroscopy (FT-IR) spectra of nano- and functionalized cellulose(s) were obtained by a standard IR spectrometer (SHIMADZU FT-IR-8400) in the range of 400–4000 cm^{-1} (conditions: 45 scans/sample, 4 cm^{-1} resolutions, KBr pellet sampling). Field Emission Scanning Electron Microscopy (JSM-7600F) was used to obtain morphological images of MCC, NCC, and DANC. The degree of crystallinity was estimated by X-ray diffraction (XRD) patterns in an automated powder X-ray diffractometer (PANalytical Empyrean, Cu-K α radiation with conditions: $\lambda = 1.5426$ Å, 40 kV, 30 mA, $2\theta = 10^\circ - 50^\circ$, 0.02°/step, 2.0 s/step, 1.0 h/scan).

2.4. Experimental design

2.4.1. Drug binding study design

The binding of ciprofloxacin hydrochloride was studied by taking cellulose (MCC) and modified cellulose (NCC, DANC) in different reagent bottles, each containing 0.082 g of MCC (solid form), NCC (5 mL 1.64 % suspension (1.64 g/100 mL)) and DANC (6.72 mL 1.22 % suspension), respectively. The volume of NCC and DANC varied to maintain 0.082 g for each sample as the NCC and DANC suspension had different concentrations in suspension. The binding experiments were performed by varying the amount of drug added to the solution, keeping the same amount of cellulose(s). Each time, the volume of the drug added to each cellulose suspension was fixed by varying the amount of DI water. This drug and cellulose(s) suspension mixture was then vigorously shaken for 1 h at 200 rpm (G-force: 4 RCF). After 1 h, drug bounded cellulose suspension(s) were centrifuged for 10 min at 4000 rpm (G-force: 538

RCF), washed with DI water to separate the cellulose residues, and unbound the drug. The concentration of unbound drug was determined using the standard UV-spectroscopic method in a UV-Vis Spectrophotometer (SHIMADZU UV- 2600, operation: 100–900 nm). The spectrum was taken from 200 nm to 600 nm, where pure ciprofloxacin hydrochloride gave its characteristic absorbance peak at 275 nm. The drug bound to each cellulose form(s) was calculated using following relation (1),

$$\text{Drug bound} = \text{Drug added} - \text{Unbound drug (measured using UV - vis)} \quad (1)$$

Moreover, the binding capacity of each cellulose form was calculated using the following relation (2),

$$\text{Drug binding capacity} = \frac{\text{Drug bound (mg)}}{\text{Cellulose(s) used (g)}} \quad (2)$$

2.4.2. Drug release study design

To evaluate the pH-responsiveness of the drug release, 6 separate experiments were performed on each cellulose form(s) with the bound drug (same amount of bound drug on each sample; therefore amount of sample was different due to the different binding capacity of each sample) at pH values of 2.5 (simulated gastric fluid), 3.5, 6.5, 7, 8, and 8.5 (simulated intestinal fluid). To find the amount of released drug, powdered samples with the loaded drug were taken in 50 mL solution at a defined pH and slowly stirred at 20 rpm (negligible G-force to ensure little/no effects of shaking on release) for 6 h to ensure the release of the bounded drug with its natural diffusion or other mechanism. After 6 h, each suspension was centrifuged at 4000 rpm (G-force: 538 RCF) for 10 min and washed with DI to separate cellulose residue as in the previous method. The release drug was identified and determined using a UV-Vis Spectrophotometer (SHIMADZU UV- 1601, operation: 100–900 nm). The difference between the absorbance of the control (prior to drug release) and released sample (after drug release, amount of released drug was calculated from a standard calibration curve (prepared for ciprofloxacin hydrochloride).

2.4.3. Swelling study design

The swelling behavior of the excipients can be strongly correlated to the drug release response. Therefore, the water uptake capacity (g/g) of DANC was measured by a dialysis membrane sack (Zhang et al., 2020). To evaluate the variability of water uptake by DANC, 1 g of DANC was taken into the dialysis membrane bag and kept in a beaker with DI water at pH 2.5 and 8.5. After 6 h, the swelled dialysis bag was removed from the beaker and weighed upon removing extra surface water in the membrane by filter paper. The water uptake (g/g) was calculated by subtracting the weight of the initial dialysis membrane from the swelled dialysis membrane bag.

2.4.4. Drug release kinetics

To understand the in-depth correlation of time elapse and drug release, kinetic experiments were evaluated at pH 2.5 and 8.5 for MCC, NCC and DANC. For pH 2.5, time variations were set as 1 to 6 h with each data point at 1 h interval. For pH 8.5, time variation was small (5–60 min). The release profile of the drug at pH 2.5 was evaluated utilizing different kinetic models. As at pH 2.5, drug release was slow enough, which demanded kinetic evaluation. However, at pH 8.5, release was much faster; for fast release, fittings of kinetic models can lead to confusing results. Therefore, pH 8.5 was not taken into consideration for kinetic study. Each mathematical model is based on different theories (basic to advanced) and can be used to demonstrate drug release from dosage forms. Different factors influence drug release, e.g., drug nature, solution properties, and characteristics of excipients. In our study, the kinetics of ciprofloxacin release from MCC, NCC, and DANC at pH 2.5 was evaluated using four widely used kinetic models, e.g., zero-order, first-order, Higuchi, and Korsmeyer–Peppas to unveil the inherent

mechanism of ciprofloxacin release from different forms of cellulose.

The zero-order release model can be defined as the following equation (3) (Laracuent et al., 2020),

$$Q_t = Q_0 + K_0 t \quad (3)$$

Where Q_t is the amount of drug released within time t , Q_0 is the initial amount of drug in the solution, which is 0 in our case, and K_0 is the zero-order release constant. The zero order release model is valid for systems where the release rate of a drug is independent of the amount of drug remaining in the delivery system.

The first-order release model can be defined as the following equation (4) (Mulye and Turco, 1995),

$$\log C = \log C_0 - \frac{K_1 t}{2.303} \quad (4)$$

Where C_0 is the initial concentration of the drug, and K_1 is the first-order constant. According to first-order release kinetics, the dissolution of a drug is correlated and dependent on the remaining drug load in the excipients.

Higuchi's model of drug release can be defined as the following equation (5) (Higuchi, 1961),

$$Q_t = K_H t^{0.5} \quad (5)$$

Where Q_t is the cumulative amount of drug released at time t , K_H is the Higuchi constant. Higuchi's model describes drug release as a diffusion process based on Fick's law. It can describe the release of different types of drugs, e.g., water-soluble, poorly water-soluble, and semi-solid drug.

The release kinetics was validated using Korsmeyer–Peppas model to understand the in-depth nature of the drug release from DANC. Korsmeyer et al. (1983) used a simple equation to describe the general solute release behavior from a controlled release polymer system equation (Korsmeyer et al., 1983), which is defined as the following equation (6),

$$\frac{M_t}{M_\infty} = K_m t^n \quad (6)$$

where M_t/M_∞ is the fraction of drug released at time t , K_m is the kinetic constant and n is the diffusion or release exponent. Herein, n is estimated from linear regression of $\log(\frac{M_t}{M_\infty})$ versus t (h). The value of n can indicate the release mechanism of drug. If the value of n is less than 0.45, it indicates quasi-fickian, where $0.45 < n < 0.89$ indicates anomalous diffusion or non-fickian diffusion; n value greater than 0.89 to less than 1 indicates the similar phenomenon of zero-order release. When $n > 1$, it indicates time-independent drug release (zero-order). Typically, when the n values reside within 0.5 to 1, diffusion and swelling of the matrix both take place. This model can predict well the release behavior of drugs from the hydrophilic matrix. Both erosion-controlled release rate and diffusion release rate influence this equation. Swellable and erodible polymers mostly follows it.

3. Results and discussion

3.1. Preparation of NCC and DANC from MCC

Fig. 1 represents the synthesis scheme of NCC and DANC. MCC generally consists of two regions, e.g., crystalline (higher density) and amorphous (lower density). When MCC is hydrolyzed (by H_2SO_4 treatment), hydronium ions (H_3O^+) migrate to the amorphous region due to the lower density of this region compared to the compact crystalline region (de Souza Lima and Borsali, 2004, Arcot et al., 2014). When H_3O^+ ions get in contact with the glycosidic linkages of MCC, hydrolytic cleaving occurs in these linkages, and individual cleaved crystallites of cellulose with nano- dimension releases. However, these cleaved nano-crystallites can aggregate. Thus, ultrasonication was applied to break down the aggregates, and stable NCC was obtained (Bondeson et al.,

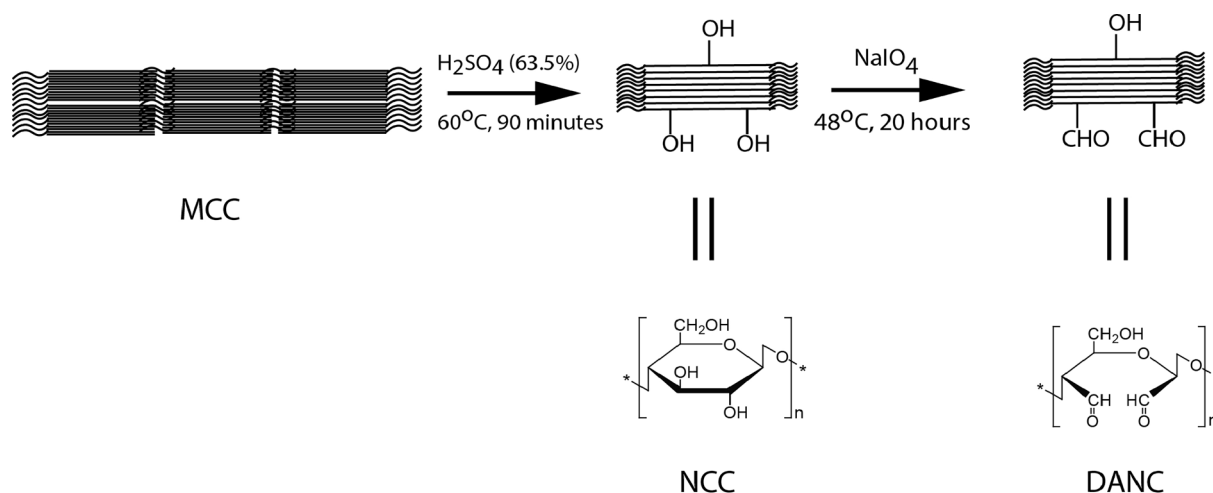


Fig. 1. Synthesis scheme and structures of DANC from MCC via NCC.

2006). Later, NCCs were subjected to periodate (NaIO_4) treatment. NCCs have three hydroxyl ($-\text{OH}$) groups in individual structures at C-2, C-3, and C-6. After NaIO_4 treatment, $-\text{OH}$ groups at C-2 and C-3 positions of NCCs were oxidized to aldehyde ($-\text{CHO}$) groups. Moreover, the corresponding C–C bond of the D-glucopyranose ring was also segregated to form 2, 3- dialdehyde cellulose (DANC). The extent of functionalization is sensitive to the concentration of periodate, reaction time, and temperature. After the desired functionalization, the reaction was stopped by reducing the excess periodate by ethylene glycol.

3.2. Characterizations

The conversion of NCC to form DANC was confirmed using the standard 2, 4- dinitrophenylhydrazine (2, 4-DNPH) test, which is typically used to qualitatively detect the carbonyl groups ($\text{C} = \text{O}$) associated with aldehydes and ketones. The reaction of 2, 4-DNPH, and $\text{C} = \text{O}$ groups form an indicative yellow or orange dinitrophenylhydrazone precipitate. After adding 2, 4-DNPH in the dilute aqueous suspension of NCC and DANC, the observed color change is represented in Figure S1. The NCC suspension turned into turbid greenish-yellow due to the insolubility of NCC in aqueous solution. However, the suspension of DANC formed an orange precipitate, which exhibited the confirmation of the characteristic reaction of the aldehyde with the reagent to form a hydrazone product.

In the spectroscopic analysis of NCC and DANC (Fig. 2(A)), peaks associated with the stretching and bending vibrations of $-\text{OH}$ groups can be visible at 3400 cm^{-1} (broad and centered) and 1300 cm^{-1} (narrow) (Yuen et al., 2009). The peak intensities (at 3400 cm^{-1} and 1300 cm^{-1}) were significantly reduced in DANC, confirming that OH groups of NCC structure were converted into other groups. In both NCC and DANC, $-\text{C}-\text{H}$ stretching vibrations (2900 cm^{-1}), $>\text{CH}_2$ bending and scissoring (1430 cm^{-1}), and ether (R-O-R) stretching vibrations (1020 cm^{-1}) were detected (Habibi et al., 2010), which is evident that parent structure of NCC was preserved after selective oxidation (in DANC).

However, due to the free aldehydes ($-\text{CHO}$), DANC showed a weak peak at 1740 cm^{-1} (Motiur Rahman et al., 2021). The low intensity of $-\text{CHO}$ groups in the DANC structure may be attributed to the degree of oxidation being not very significant, which indicates further oxidation of DANC may induce more changes in the functional groups. However, these peaks (associated with $-\text{CHO}$ groups) are very tough to identify due to moisture availability in the structure. Spedding et al. (1960) reported that dried oxidized cellulosic samples (e.g., DANC) showed several forms of combined aldehyde grouping, e.g., hydrated aldehyde, hemiacetal, etc. (Spedding, 1960). The presence of hemiacetal can be confirmed by the peak at around 900 cm^{-1} , which was also observed in

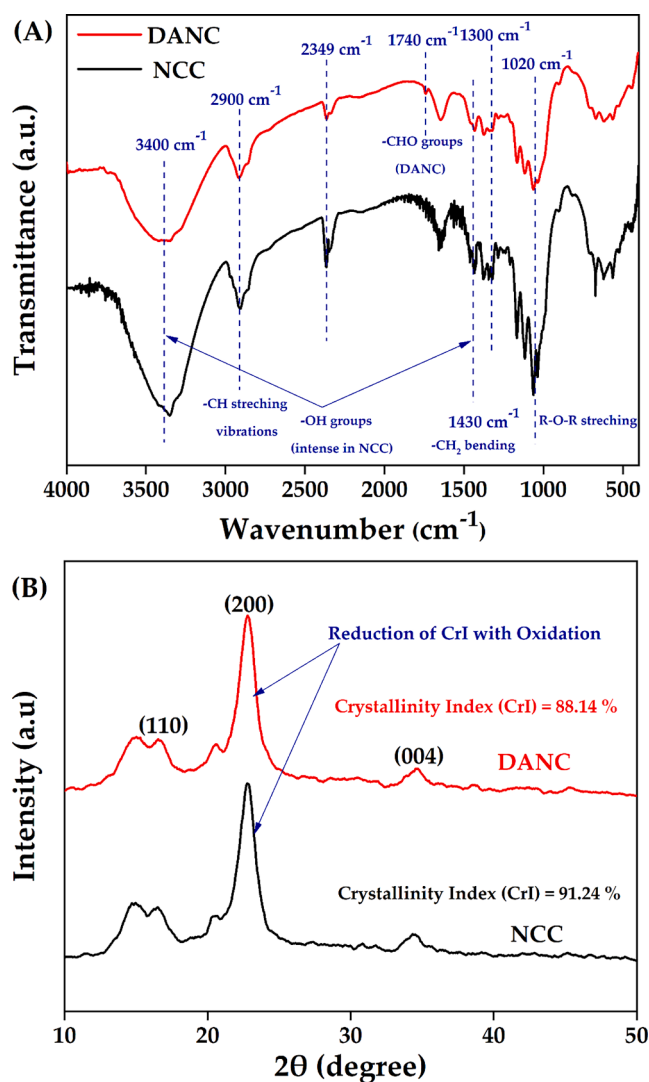


Fig. 2. FT-IR spectra (with characteristic peaks) (A), and XRD analysis (with characteristic plane) (B) of NCC and DANC.

both NCC and DANC. It suggests further oxidation of DANC may result in the disappearance of such a peak. This phenomenon was described by the previous researcher(s) as well. Motiur Rahman et al. (2021) reported further oxidation of DANC to form carboxylated nanocellulose, resulting in the disappearance of hemiacetal peaks (Motiur Rahman et al., 2021). However, the exact degree of oxidation due to the formation of DANC may not be evident from FT-IR spectroscopy, as FT-IR can hardly detect carbonyl groups due to the hydration and acetalization effects (Keshk, 2008). The absorption peak around 2349 cm^{-1} has been traced due to atmospheric CO_2 during the experiment.

The surface morphologies of MCC, NCC, and DANC were investigated by FESEM (Figure S2). MCC particles were of irregular and scattered shapes (average diameter $\sim 10\text{--}50\ \mu\text{m}$). The diameter of NCC significantly reduced compared to MCC (width within the range of $100\text{--}300\ \text{nm}$) (Dong et al., 1998). In nano form, intermolecular H-bonding and hydrophilic interaction within crystallite nanocellulose chains formed an agglomerated compact structure for NCC. The NCC demonstrated a needle-shaped fibrous form. The width of DANC was identical to NCC, however DANC exhibited leaf-like stack laminar-rectangular structure with characteristic nano-size dimensions (Motiur Rahman et al., 2021).

The change in crystalline behavior during the selective oxidation of NCC was evaluated by XRD analysis (Fig. 2(B)). The characteristic peaks (responsible for conventional cellulose structure) were observed at 18° (110 plane), 22.5° (200 plane) and 34.4° (040 plane) (Mohamed et al., 2017). To get the quantitative indicator of crystallinity of NCC and DANC, relative crystallinity index (CrI) was calculated. It indicates the relative amount of crystalline (ordered) and amorphous (disordered) phases in cellulose materials. CrI of NCC and DANC was calculated according to the amorphous subtraction and can be defined as equation (7),

$$CrI = \frac{I_{\text{main}} - I_{\text{am}}}{I_{\text{main}}} \times 100 \quad (7)$$

Here, I_{main} is the maximum intensity at the main peak, which is 002 plane; therefore, I_{main} is I_{002} . At the 002 peak maximum near $2\theta = 22.5^\circ$. I_{am} is the intensity of diffraction in the same units at $2\theta = 18^\circ$. The calculated CrI for NCC was 91.24 %, whereas for DANC, it was 88.14 %. The conversion of cellulose degrades and weakens the hydrogen bonding during the oxidation process, which may decrease the CrI, as with increasing CrI, the strength of the polymer increases due to enhanced intermolecular bonding in the crystalline phase. Moreover, C-2 and C-3 oxidation exposed the glucopyranose rings of NCC and destroyed its ordered packing. Previously, Kim et al. (2020) reported the phenomenon of CrI decrease with the degree of oxidation of the cellulose chain (Kim et al., 2000).

3.3. Drug binding study

The binding of ciprofloxacin hydrochloride was evaluated on MCC, NCC, and DANC at the pH of deionized water ($\text{pH} = 6.5$). In each case, the desired amount of drug was mixed with solutions of different forms of cellulose (MCC, NCC, and DANC) of fixed volume. It is evident from Fig. 3(A) that the amount of drug bound increases with the rise of drug concentration. At lower drug concentrations, the driving force between drug particles and the surface of MCC, NCC, and DANC was low, which increased with increasing drug concentration. However, after a particular drug concentration, the binding of the drug entered a stabilized zone, where the rate of drug binding started to decrease and reached an equilibrium. The saturation of binding sites of cellulose and modified cellulose hindered the further uptake of drug after a certain drug concentration (Patra et al., 2018, Ciolacu et al., 2020). The release phenomenon was the primary concern of the study; therefore, the binding of the drug was not studied as a function of time. It is likely to assume that drug binding can vary with time (Münster et al., 2019); however, in our

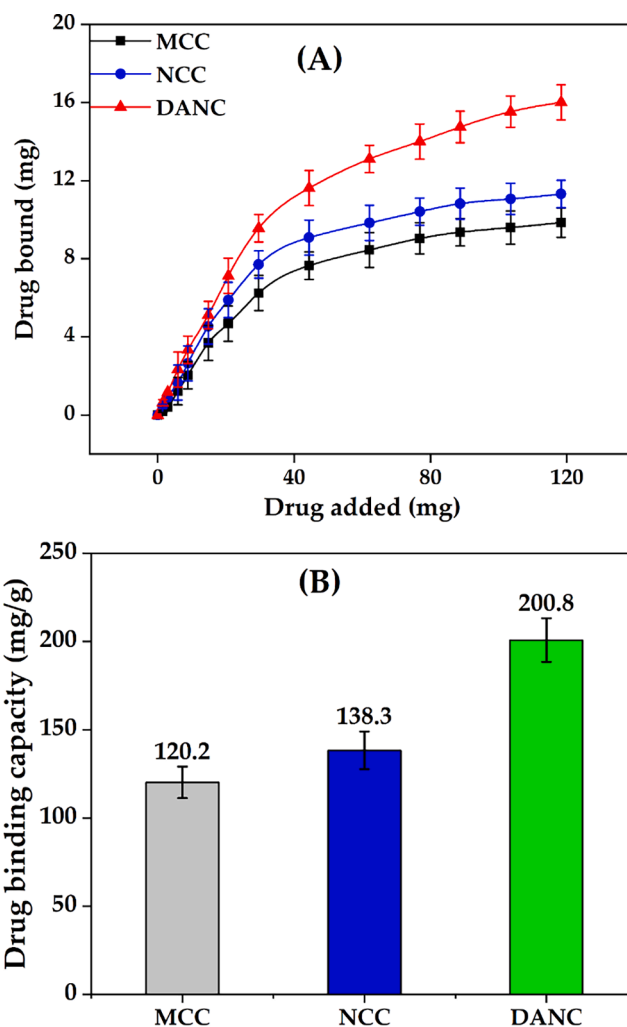


Fig. 3. Drug bound vs Drug added relationship (A) and drug binding capacity (B) of micro-, nano- and di-aldehyde nanocrystalline cellulose.

study, it was fixed (1 h).

After 1 h, the binding capacity of DANC was found to be 200.8 mg/g, whereas for NCC and MCC, the binding capacities were 138.3 and 120.2 mg/g (Fig. 3(B)). The H_2SO_4 hydrolysis of MCC induced a greater surface area in NCC moreover due to the dimensional effects, active sites ($-\text{OH}$ groups) of NCC were more exposed to binding with drug particles compared to MCC (Alavi, 2019, Mamudu et al., 2023). Therefore, a higher binding of ciprofloxacin hydrochloride occurred in the NCC compared to MCC. The oxidized C-2 and C-3 of DANC attracted ciprofloxacin more strongly compared to NCC. The interaction of ciprofloxacin, specifically the amine groups ($-\text{NH}_2$) of ciprofloxacin hydrochloride with two aldehydes ($-\text{CHO}$) groups of DANC, was strong enough to attach a higher number of ciprofloxacin compared to the hydroxyl ($-\text{OH}$) groups of NCC (Sahoo et al., 2011). Moreover, the drug binding experiment was executed at pH 6.5; at this pH, $-\text{NH}_2$ groups of ciprofloxacin may turn into $-\text{NH}_2^+$, which elevated the attraction between the oxygenated functional groups of DANC and ciprofloxacin (Kooti et al., 2018). In addition, the rod-shaped agglomerated DANC structure provided several active sites for physical interaction to bind drug particles.

3.4. pH-responsive release study

The pH-responsiveness of a particular drug release phenomenon is crucial for considering the real-life application of an excipient.

Therefore, ciprofloxacin hydrochloride release from MCC, NCC, and DANC was studied at five different pHs within pH 2.5 to 8.5 for 6 h. The range of 2.5–8.5 somehow reflects the actual pH range of the human gastrointestinal tract from the stomach to the small intestine. The average time of gastrointestinal journey is 6–8 h. Thus, the study was conducted for 6 h.

At low pH, the release was low for all cellulose(s) forms. The amount of released drug increased with the increase of pH for all cellulose samples (Fig. 4(A)). After 6 h, at pH 2.5, for per gram of MCC, NCC, and DANC, amounts of released drug were 5.02, 5.52, and 7.02 mg, whereas at pH 8.5, released drug amounts 8.13, 8.82, 13.18 mg, respectively. For the whole pH range (2.5–8.5), DANC exhibited the highest amount of drug release compared to NCC and MCC. However, the amount of drug released may not clearly present the scenario. Therefore, the extent of release (ratio of drug released to drug bound) was presented for MCC, NCC, and DANC at pH 8.5 (Fig. 4(B)). At acidic pH, the extents of release were very moderate, ranging from 9.63 to 23.3 % (MCC), 11.2–28.8 % (NCC), and 18.5–44.8 % (DANC) however it arose rapidly when the pH entered basic region, and for DANC it reached up to 84.8 % at pH 8.5, while NCC and MCC showed extent of release of around 45.1 % and 37.7 % within 10 min. The higher extent of drug release for DANC compared to NCC and MCC may be attributed to the fact that the sites of DANC bound with drug particles were reversible, which indicates repeatable use of DANC as a drug carrier. Moreover, the resistance of NCC and MCC to release drugs can be attributed to the irreversible binding of drugs with these forms of cellulose(s). The structure and interactions of ciprofloxacin at acidic and basic pH are presented in Fig. 5. At lower pH, the low extent of release for modified cellulose possibly occurred due to several factors, e.g., i) at acidic pH ($\text{pH} = 2.5$), ciprofloxacin hydrochloride becomes cationic (Fig. 5); due to the availability of H^+ ions, structure of ciprofloxacin becomes protonated ($-\text{NH}_2$ becomes $-\text{NH}_2^+$) (Kooti et al., 2018), which strengthen the interaction of drug molecules with oxygenated functional groups of modified cellulose (stabilized drug/carrier interaction), thus release was hindered (Valdés et al., 2017), ii) at low pH, swelling of MCC, NCC and DANC was low, thus, drug particles diffused through the nanosized scattered and irregular pores of these modified cellulose(s) and then solubilized in the solution, which delayed and limited the drug release, whereas at basic pH ($\text{pH} = 8.5$), ciprofloxacin becomes anionic ($-\text{COOH}$ to $-\text{COO}^-$) (Kooti et al., 2018), which conflicts with oxygenated functional groups of cellulose (s), therefore released rapidly (Fig. 5). Moreover, at basic pH, swelling or erosion accelerated the release of drug particles.

3.5. Swelling study

To understand the swelling behavior of DANC, the water absorption or uptake capacity of DANC was evaluated at pH 2.5 and pH 8.5 at variable times ranging from 5 min to 6 h (Fig. 4 (C)). At pH 2.5, after 1 h, the water uptake of DANC was 1.4 g/g, which reached an equilibrium after 6 h with a saturated water capacity of 4 g/g. However, at pH 8.5, water uptake capacity was relatively high and fast. Interestingly, within a very short time (10 min), it reached equilibrium with 7.45 g/g uptake. The water uptake behavior of C-2 and C-3 functionalized cellulose can be correlated to the drug release behavior. At basic pH, entropy-induced conformational changes, and dissociable functional groups attracted water molecules. Therefore, water molecules entered into the DANC structure. Moreover, nature to minimize electrical charges in a single structure expanded DANC structure and enhanced water uptake (Motiur Rahman et al., 2021).

3.6. Kinetics of release

The time dependence of drug release is a crucial concern to design a controlled drug delivery system (Geraili et al., 2021). The release of ciprofloxacin hydrochloride from MCC, NCC, and DANC was studied at pH 2.5 for 6 h (Fig. 6 (A)) and at pH 8.5 for 1 h (Fig. 6(B)). The time scales

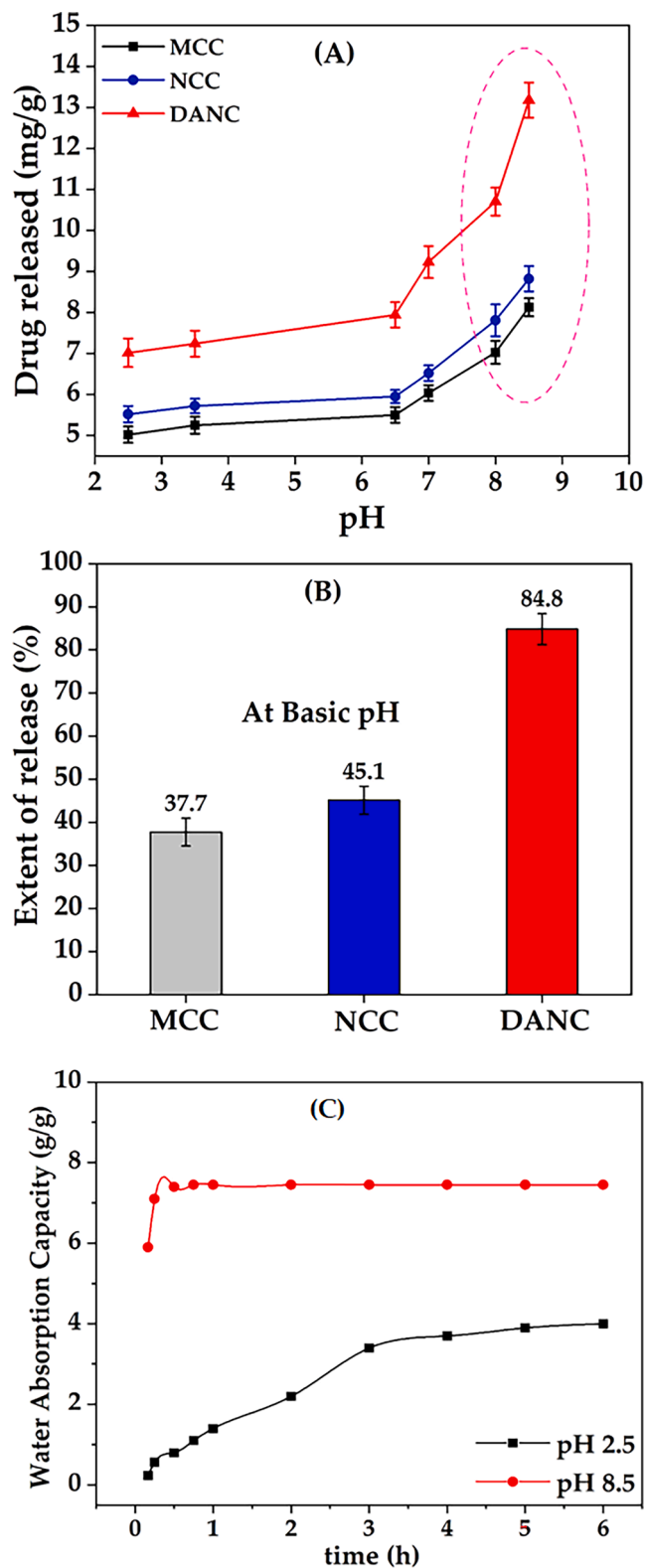


Fig. 4. Drug release as a function of time (A), extent of release at pH 8.5 (B) for MCC, NCC, and DANC, water absorption or uptake (g/g) as a function of time for DANC at pH 2.5 and pH 8.5.

were different for pH 2.5 (h) and pH 8.5 (min), based on the slow release at pH 2.5 and fast release at pH 8.5. The selection of the time range was based on the swelling behavior described in Fig. 4 (C). At pH 2.5, the release of the drug was prolonged, and it took 6 h to reach an approximate equilibrium, and the extents of release were 23.3, 28.8, and 44.8

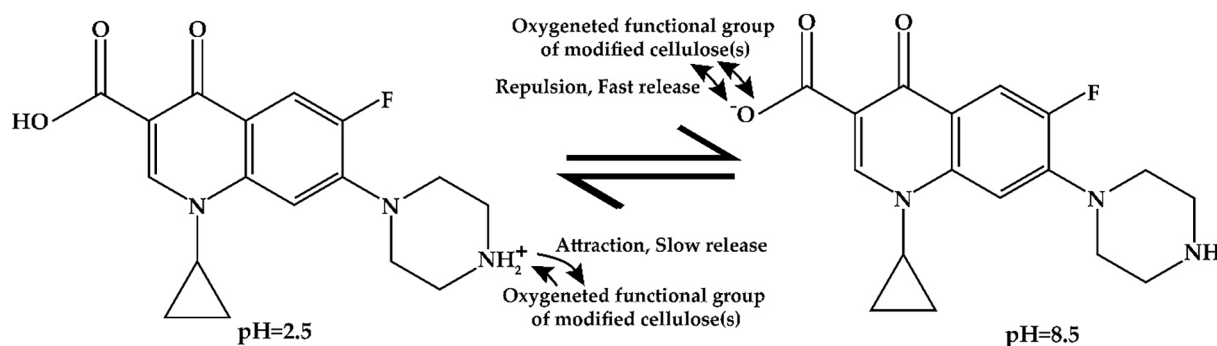


Fig. 5. The structure and interactions of ciprofloxacin at pH 2.5 and pH 8.5.

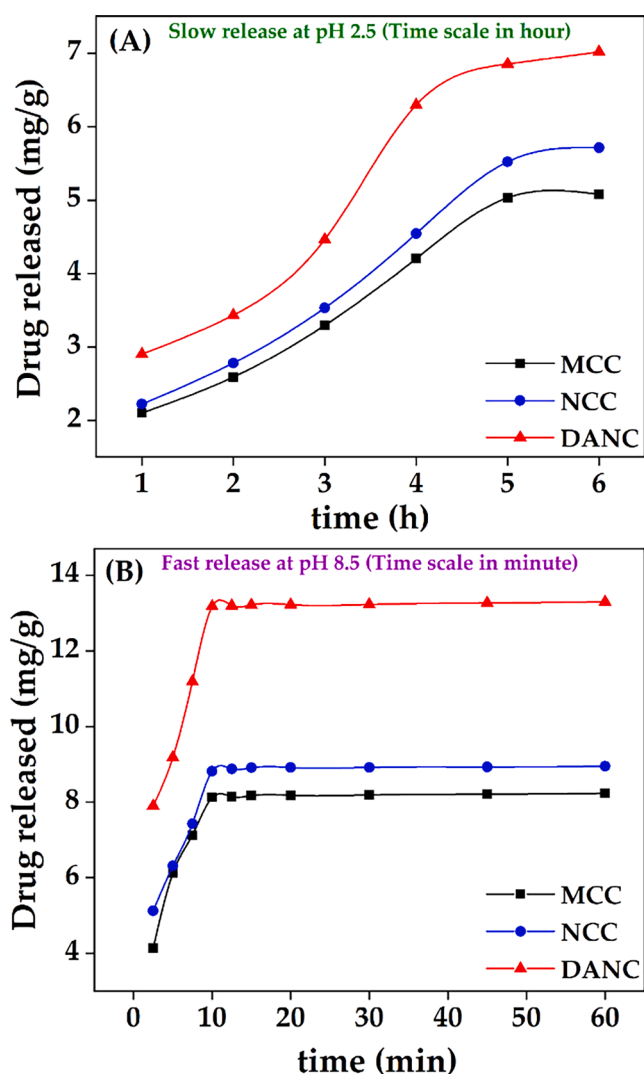


Fig. 6. Release of ciprofloxacin hydrochloride at pH 2.5 (A), and pH 8.5 (B) from MCC, NCC, and DANC at different time scales (hour for pH 2.5 and minute for pH 8.5).

% for MCC, NCC, and DANC, respectively.

At pH 8.5, within 10 min, extent of drug released for DANC crossed 84 %. There were no significant changes in release after 10 min. The rapid release of the drug at pH 8.5 can be reflected by the water uptake capacity of DANC (Fig. 4(C)). The exchange of ciprofloxacin with water can be a possible reason indicating the polyelectrolyte nature of DANC. The average time of the gastrointestinal tract journey of food processing

is 6–8 h (Sensoy, 2021). Therefore, the release of drugs at lower pH would be slow.

The drug release was slow at pH 2.5; thus, to understand the in-depth release mechanism, the kinetics of the release were evaluated using different kinetic models. As release at pH 8.5 was much more rapid, the release of the drug was mostly influenced by the sudden swelling of the matrix at basic pH (Fig. 4(C)). An ideal controlled drug release system initially releases a fraction of the drug to attain a moderate therapeutic efficacy and then releases other portions with the requirement (Wang et al., 2020). Controlled drug delivery systems maintain a certain drug dose in the excipients to release at specific interval (Sreedharan and Singh, 2019). The ciprofloxacin hydrochloride release from MCC, NCC, and DANC at pH 2.5 was validated using different kinetic models, e.g., zero-order, first-order, Higuchi model, and Korsmeyer–Peppas model (Fig. 7). Zero-order kinetics showed a good correlation coefficient (R^2) for MCC (0.97), NCC (0.97), and DANC (0.96) (Fig. 7(A)). The K_0 values are 4.51, 5.45, and 8.71. According to the zero-order model, the release of the drug is independent of the dose present in the excipients and accounts for the slow release. At pH 2.5, the release was slow enough to be considered a constant release rate. Thus zero order kinetics fitted well with the release kinetics. However, Fig. 4(B) shows that the drug release rate was comparatively higher in the first 4 h and then stabilized between 4 and 6 h. However, fittings for first-order were also good, with R^2 values ranging from 0.93 (DANC) to 0.96 (NCC) (Fig. 7(B)). First-order release is dependent on the drug dose available on the carrier. Thus, release from these cellulose-based carriers at pH 2.5 may follow a complex mechanism which next two models can validate. The fitting precision was found to be highest for the Higuchi kinetics model, R^2 was 0.99 for all the cellulose forms (Fig. 7(C)). The K_H values were 18.40, 11.35, and 9.45 for DANC, NCC, and MCC, respectively. Higuchi (1961) proposed this kinetic model to describe drug release from a matrix system (DANC is a matrix) (Higuchi, 1961). Higuchi kinetic model assumes that the drug diffusivity is constant and unidirectional, which is valid only when excipient matrices do not swell significantly in aqueous solution (2015). The swelling of the DANC matrix at pH 2.5 was too low and sluggish, which justifies the assumption of the Higuchi model. Moreover, the Higuchi model consists of the contribution of dissolution and diffusion. It considers the release of drugs in the environment, which maintains perfect sink conditions (Siepmann and Siepmann, 2020). In general, the perfect sink condition is obtained when the total dissolution of drug molecules attains a final concentration that is significantly lower than the saturated solution, and it enhances the driving force of dissolution, which is valid in our case (Hermans et al., 2022). This model worked as the basis for the development of other improved models, like the Korsmeyer and Peppas model (Korsmeyer et al., 1983). For evaluating the types of diffusion, release data were validated by the Korsmeyer–Peppas model. The fittings of the Korsmeyer–Peppas equation were in good agreement (Fig. 7(D)); the R^2 values for DANC, NCC, and MCC were 0.95, 0.95, and 0.92. The values of ciprofloxacin hydrochloride release exponent (n) were 0.54, 0.57, and 0.55. The value of

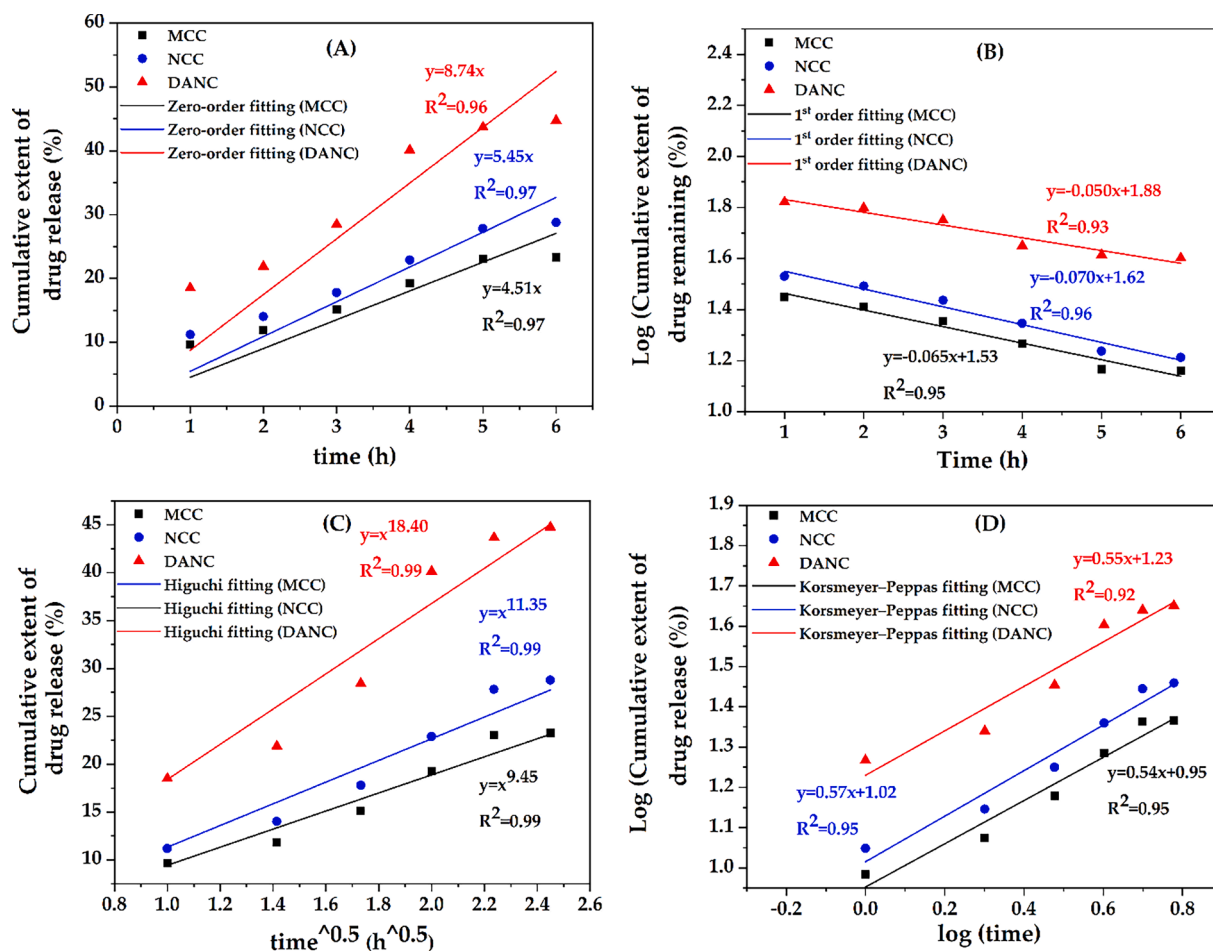


Fig. 7. Kinetic results of zero order (A), 1st order (B), Higuchi (C), and Korsmeyer-peppas (D) models for MCC, NCC, and DANC.

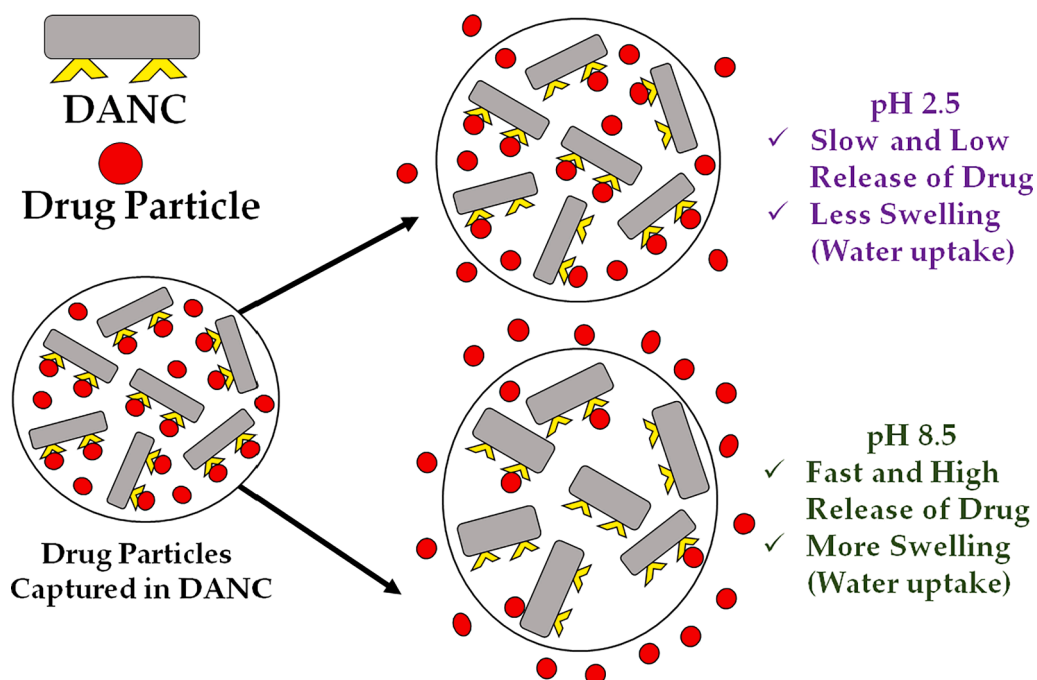


Fig. 8. Release phenomenon of ciprofloxacin hydrochloride from DANC matrix at pH 2.5 and pH 8.5.

n can indicate the release mechanism of the drug. Since the n values were found between 0.45 and 0.89 for all the ciprofloxacin/excipient systems, it indicates that the release was controlled by non-fickian diffusion (Permanadewi et al., 2019). Thus, polymer relaxation time was not more significant than the characteristic solvent diffusion time. It implies that diffusion, dissolution, swelling (at pH 2.5, it was minimal) and slight erosion all contributed to the drug release in our case. As all the excipients were hydrophilic matrices, the Korsmeyer-Peppas model predicted quite well (Hiremath and Saha, 2008). The release rate may include diffusion release, erosion release, and erosion release rate. The phenomenon of slow release over 6 h at pH 2.5 and rapid release within 10 min at pH 8.5 (Fig. 8) can be used to design controlled drug delivery, where after a certain time, a significant dosage release is required, and for a long time sustained release is required.

4. Conclusion

Nanocrystalline cellulose and di-aldehyde nanocrystalline cellulose were successfully synthesized from microcrystalline cellulose by sequential acid hydrolysis and selective oxidation. The prepared materials were characterized, and conversion was confirmed through the 2,4-DNPH test, FT-IR, FESEM, and XRD. DANC exhibited the highest binding capacity (208.8 mg/g) for ciprofloxacin hydrochloride, possibly due to its exposed structure, enhanced interaction sites, and interactable functional groups in the DANC. The release of the drug was highly dependent on pH. At acidic pH, release was prolonged, which increased with increasing pH. At pH 2.5, after 6 h, MCC, NCC, and DANC released 23.3, 28.8 %, and 44.8 % of loaded drugs. However, at pH 8.5, the extent of release(s) (compared to the loaded drug) were 84.8, 45.1 and 37.7 % within 10 min for DANC, NCC, and MCC, respectively. Water uptake capacity (g/g) of DANC showed an identical trend of drug release, slow and low (4 g/g) at pH 2.5 and fast and high (7.45 g/g) at pH 8.5. The kinetic analysis of drug release suggested the Higuchi model ($R^2 = 0.99$ for all excipients) to interpret the drug release behavior at pH 2.5. The swelling of the DANC matrix at pH 2.5 was low and sluggish, which justifies the assumption of the Higuchi model. The release may consist of the contribution of simultaneous dissolution and diffusion. Moreover, from the Korsmeyer-Peppas model, n values were between 0.45 and 0.89, which indicates release was also controlled by non-fiction diffusion. However, this study lacks the actual representation of the pH of the whole gastrointestinal tract. Moreover, to make this study more realistic, release kinetics from compressed DANC has to be considered rather than powdered samples. Still, the interesting nature of the DANC/ciprofloxacin system should be taken as a hope for these synthesized materials to be applied in the controlled (at stomach) and rapid (at lower intestine or basic pH environment) drug delivery, referring to extended-release or pulsatile-release of target drug products as they are programmed and shows the possible importance of the present work for further development in the relevant field in the near future.

CRedit authorship contribution statement

Hridoy Roy: Conceptualization, Data curation, Formal analysis, Investigation, Methodology, Validation, Visualization, Writing – original draft, Writing – review & editing. **Khalide Hasan Parvej:** Conceptualization, Data curation, Investigation, Writing – original draft. **Mohammad Mozammel Hosen:** Conceptualization, Investigation, Writing – original draft. **Md. Shahinoor Islam:** Funding acquisition, Project administration. **Shakhawat H. Firoz:** Conceptualization, Formal analysis, Funding acquisition, Project administration, Resources, Supervision, Validation, Writing – review & editing.

Declaration of competing interest

The authors declare that they have no known competing financial interests or personal relationships that could have appeared to influence

the work reported in this paper.

Acknowledgments

The authors would like to acknowledge the support from Bangladesh University of Engineering and Technology, Dhaka-1000, Bangladesh.

Appendix A. Supplementary data

Supplementary data to this article can be found online at <https://doi.org/10.1016/j.arabjc.2024.105763>.

References

- Ahmad, A., Mubarak, N.M., Naseem, K., et al., 2020. Recent advancement and development of chitin and chitosan-based nanocomposite for drug delivery: critical approach to clinical research. *Arab. J. Chem.* 13, 8935–8964. <https://doi.org/10.1016/j.arabjc.2020.10.019>.
- Alavi, M., 2019. Modifications of microcrystalline cellulose (MCC), nanofibrillated cellulose (NFC), and nanocrystalline cellulose (NCC) for antimicrobial and wound healing applications. *e-Polymers* 19, 103–119. <https://doi.org/10.1515/epoly-2019-0013>.
- Anis Yohana, C., Sriwidodo, S., Marline, A., 2019. Microcrystalline cellulose as pharmaceutical excipient. *pharmaceutical formulation design*. A. Usama and a. Juber. Rijeka, IntechOpen: Ch. 3.
- Arcot, L.R., Lundahl, M., Rojas, O.J., et al., 2014. Asymmetric cellulose nanocrystals: thiolation of reducing end groups via NHS-EDC coupling. *Cellul.* 21, 4209–4218. <https://doi.org/10.1007/s10570-014-0426-9>.
- Bondeson, D., Mathew, A., Oksman, K., 2006. Optimization of the isolation of nanocrystals from microcrystalline cellulose by acid hydrolysis. *Cellul.* 13, 171–180. <https://doi.org/10.1007/s10570-006-9061-4>.
- Ciolacu, D.E., Nicu, R., Ciolacu, F., 2020. Cellulose-based hydrogels as sustained drug-delivery systems. *Journal* 13. <https://doi.org/10.3390/ma13225270>.
- Crowley, M.M., Schroeder, B., Fredersdorf, A., et al., 2004. Physicochemical properties and mechanism of drug release from ethyl cellulose matrix tablets prepared by direct compression and hot-melt extrusion. *Int. J. Pharm.* 269, 509–522. <https://doi.org/10.1016/j.ijpharm.2003.09.037>.
- de Souza Lima, M.M., Borsali, R., 2004. Rodlike cellulose microcrystals: structure, properties, and applications. *Macromol. Rapid Commun.* 25, 771–787. <https://doi.org/10.1002/marc.200300268>.
- Dong, X.M., Revol, J.-F., Gray, D.G., 1998. Effect of microcrystallite preparation conditions on the formation of colloid crystals of cellulose. *Cellul.* 5, 19–32. <https://doi.org/10.1023/A:1009260511939>.
- Edgar, K.J., 2007. Cellulose esters in drug delivery. *Cellul.* 14, 49–64. <https://doi.org/10.1007/s10570-006-9087-7>.
- Gao, J., Karp, J.M., Langer, R., et al., 2023. The future of drug delivery. *Chem. Mater.* 35, 359–363. <https://doi.org/10.1021/acs.chemmater.2c03003>.
- Geralli, A., Xing, M., Mequanint, K., 2021. Design and fabrication of drug-delivery systems toward adjustable release profiles for personalized treatment. *VIEW*. 2, 20200126. <https://doi.org/10.1002/VIW.20200126>.
- Gharbani, P., 2017. Synthesis of polyaniline-tin(II)molybdo-phosphate nanocomposite and application of it in the removal of dyes from aqueous solutions. *J. Mol. Liq.* 242, 229–234. <https://doi.org/10.1016/j.molliq.2017.07.017>.
- Gharbani, P., Mehrizad, A., Jafarpour, I., 2015. Adsorption of penicillin by decaffeinated tea waste. *Pol. J. Chem. Technol.* 17, 95–99. <https://doi.org/10.1515/pjct-2015-0056>.
- Gharbani, P., Mehrizad, A., Mosavi, S.A., 2022. Optimization, kinetics and thermodynamics studies for photocatalytic degradation of methylene blue using cadmium selenide nanoparticles. *npj Clean Water*. 5, 34. <https://doi.org/10.1038/s41545-022-00178-x>.
- Habibi, Y., Lucia, L.A., Rojas, O.J., 2010. Cellulose nanocrystals: chemistry, self-assembly, and applications. *Chem. Rev.* 110, 3479–3500. <https://doi.org/10.1021/cr900339w>.
- Heinze, T., El Seoud, O.A., Koschella, A., 2018. Etherification of cellulose. In: Heinze, T., El Seoud, O.A., Koschella, A. (Eds.), *Cellulose Derivatives: Synthesis, Structure, and Properties*. Publishing, Cham, Springer International, pp. 429–477.
- Hermans, A., Milsman, J., Li, H., et al., 2022. Challenges and strategies for solubility measurements and dissolution method development for amorphous solid dispersion formulations. *AAPS J.* 25, 11. <https://doi.org/10.1208/s12248-022-00760-8>.
- Higuchi, T., 1961. Rate of release of medicaments from ointment bases containing drugs in suspension. *J. Pharm. Sci.* 50, 874–875. <https://doi.org/10.1002/jps.2600501018>.
- Hiremath, P.S., Saha, R.N., 2008. Controlled release hydrophilic matrix tablet formulations of isoniazid: design and in vitro studies. *AAPS PharmSciTech* 9, 1171–1178. <https://doi.org/10.1208/s12249-008-9159-0>.
- Hossain, M.A., Roy, C.K., Sarkar, S.D., et al., 2020. Improvement of the strength of poly (acrylic acid) hydrogels by the incorporation of functionally modified nanocrystalline cellulose. *Materials Advances*. 1, 2107–2116. <https://doi.org/10.1039/D0MA00478B>.
- Jackson, J.K., Letchford, K., Wasserman, B.Z., et al., 2011. The use of nanocrystalline cellulose for the binding and controlled release of drugs. *IJN*. 321 <https://doi.org/10.2147/IJN.S16749>.

- Keshk, S.M.A.S., 2008. Homogenous reactions of cellulose from different natural sources. *Carbohydr. Polym.* 74, 942–945. <https://doi.org/10.1016/j.carbpol.2008.05.022>.
- Kim, U.-J., Kuga, S., Wada, M., et al., 2000. Periodate oxidation of crystalline cellulose. *Biomacromolecules* 1, 488–492. <https://doi.org/10.1021/bm0000337>.
- Kooti, M., Sedeh, A.N., Motamedi, H., et al., 2018. Magnetic graphene oxide inlaid with silver nanoparticles as antibacterial and drug delivery composite. *Appl. Microbiol. Biotechnol.* 102, 3607–3621. <https://doi.org/10.1007/s00253-018-8880-1>.
- Korsmeyer, R.W., Gurny, R., Doelker, E., et al., 1983. Mechanisms of solute release from porous hydrophilic polymers. *Int. J. Pharm.* 15, 25–35. [https://doi.org/10.1016/0378-5173\(83\)90064-9](https://doi.org/10.1016/0378-5173(83)90064-9).
- Laracunte, M.-L., Yu, M.H., McHugh, K.J., 2020. Zero-order drug delivery: state of the art and future prospects. *J. Control. Release* 327, 834–856. <https://doi.org/10.1016/j.jconrel.2020.09.020>.
- Li, Z., Li, S., Yu, D., et al., 2024. Elucidating pH dynamics in Pickering emulsions stabilized by soybean protein isolate and nicotinamide mononucleotide: enhancing emulsification and curcumin delivery mechanisms. *Colloids Surf. A Physicochem. Eng. Asp.* 683, 133024 <https://doi.org/10.1016/j.colsurfa.2023.133024>.
- Li, Z., Yu, D., 2023a. Controlled ibuprofen release from Pickering emulsions stabilized by pH-responsive cellulose-based nanofibrils. *Int. J. Biol. Macromol.* 242, 124942 <https://doi.org/10.1016/j.ijbiomac.2023.124942>.
- Li, Z., Yu, D., 2023b. Formulation and characterization of pH-responsive pickering emulsions stabilized by soy protein isolate/nicotinamide mononucleotide complexes for controlled drug release. *Ind. Crop. Prod.* 203, 117158 <https://doi.org/10.1016/j.indcrop.2023.117158>.
- Mamudu, U., Hussin, M.R., Santos, J.H., et al., 2023. Synthesis and characterisation of sulfated-nanocrystalline cellulose in epoxy coatings for corrosion protection of mild steel from sodium chloride solution. *Carbohydr. Polym. Technol. Appl.* 5, 100306 <https://doi.org/10.1016/j.carpta.2023.100306>.
- Mohamed, M.A., Salleh, W.N.W., Jaafar, J., et al., 2017. Physicochemical characterization of cellulose nanocrystal and nanoporous self-assembled CNC membrane derived from Ceiba pentandra. *Carbohydr. Polym.* 157, 1892–1902. <https://doi.org/10.1016/j.carbpol.2016.11.078>.
- Motiur Rahman, M., Hasan Howlader, A., Rahman, E., et al., 2021. Development of functionalized nanocrystalline cellulose-based polyelectrolytes with high water uptake. *Polym. J.* 53, 913–921. <https://doi.org/10.1038/s41428-021-00483-1>.
- Mou, K., Li, J., Wang, Y., et al., 2017. 2,3-dialdehyde nanofibrillated cellulose as a potential material for the treatment of MRSA infection. *J. Mater. Chem. B* 5, 7876–7884. <https://doi.org/10.1039/C7TB01857F>.
- Mulye, N.V., Turco, S.J., 1995. A simple model based on first order kinetics to explain release of highly water soluble drugs from porous dicalcium phosphate dihydrate matrices. *Drug Dev. Ind. Pharm.* 21, 943–953. <https://doi.org/10.3109/03639049509026658>.
- Münster, L., Fojtů, M., Capáková, Z., et al., 2019. Selectively oxidized cellulose with adjustable molecular weight for controlled release of platinum anticancer drugs. *Biomacromolecules* 20, 1623–1634. <https://doi.org/10.1021/acs.biomac.8b01807>.
- Mura, P., Maestrelli, F., Cirri, M., et al., 2022. Multiple roles of chitosan in mucosal drug delivery: an updated review. *Journal* 20. <https://doi.org/10.3390/md20050335>.
- O'Connor, R.E., Schwartz, J.B., 1993. Drug release mechanism from a microcrystalline cellulose pellet system. *Pharm. Res.* 10, 356–361. <https://doi.org/10.1023/A:1018928003668>.
- Pachua, L., 2017. Application of nanocellulose for controlled drug delivery. *Nanocell. Nanohydr. Matrices* 1–19.
- Pal, D., Raj, K., 2023. Chapter 2 - properties of plant polysaccharides used as pharmaceutical excipients. In: Nayak, A.K., Hasnain, M.S., Pal, D. (Eds.), *Plant Polysaccharides as Pharmaceutical Excipients*. Elsevier, pp. 25–44.
- Patra, J.K., Das, G., Fraceto, L.F., et al., 2018. Nano based drug delivery systems: recent developments and future prospects. *J. Nanobiotechnol.* 16, 71. <https://doi.org/10.1186/s12951-018-0392-8>.
- Permanadewi, I., Kumoro, A.C., Wardhani, D.H., et al., 2019. Modelling of controlled drug release in gastrointestinal tract simulation. *J. Phys. Conf. Ser.* 1295, 012063 <https://doi.org/10.1088/1742-6596/1295/1/012063>.
- Pooresmaeil, M., Hassanpourghadam, Y., Namazi, H., 2023. Chitosan/carboxymethyl starch bio-coated naproxen@GQDs/Copper glutamate MOFs: a new system for colon-specific drug delivery relay on the special structure of the used polymers. *Eur. Polym. J.* 184, 111802 <https://doi.org/10.1016/j.eurpolymj.2022.111802>.
- Sahoo, S., Chakraborti, C., Mishra, S., 2011. Qualitative analysis of controlled release ciprofloxacin/carbopol 934 mucoadhesive suspension. *J. Adv. Pharm. Tech. Res.* 2, 195. <https://doi.org/10.4103/2231-4040.85541>.
- Seddiqi, H., Oliaei, E., Honarkar, H., et al., 2021. Cellulose and its derivatives: towards biomedical applications. *Cellul.* 28, 1893–1931. <https://doi.org/10.1007/s10570-020-03674-w>.
- Sensoy, I., 2021. A review on the food digestion in the digestive tract and the used in vitro models. *Curr. Res. Food Sci.* 4, 308–319. <https://doi.org/10.1016/j.crf.2021.04.004>.
- Siepmann, J., Siepmann, F., 2020. Sink conditions do not guarantee the absence of saturation effects. *Int. J. Pharm.* 577, 119009 <https://doi.org/10.1016/j.ijpharm.2019.119009>.
- Siller, M., Amer, H., Bacher, M., et al., 2015. Effects of periodate oxidation on cellulose polymorphs. *Cellul.* 22, 2245–2261. <https://doi.org/10.1007/s10570-015-0648-5>.
- Spedding, H., 1960. 628. Infrared spectra of periodate-oxidised cellulose. *J. Chem. Soc. (resumed)* 3147–3152. <https://doi.org/10.1039/JR9600003147>.
- Sreedharan, S., Singh, R., 2019. Ciprofloxacin functionalized biogenic gold nanoflowers as nanoantibiotics against pathogenic bacterial strains. *IJN.* 14, 9905–9916. <https://doi.org/10.2147/IJN.S224488>.
- Valdés, L., Pérez, L., de Ménorval, L.C., et al., 2017. A simple way for targeted delivery of an antibiotic: in vitro evaluation of a nanoclay-based composite. *PLoS One* 12, e0187879.
- Wang, S., Liu, R., Fu, Y., et al., 2020. Release mechanisms and applications of drug delivery systems for extended-release. *Expert Opin. Drug Deliv.* 17, 1289–1304. <https://doi.org/10.1080/17425247.2020.1788541>.
- Wang, Y., Wang, X., Xie, Y., et al., 2018. Functional nanomaterials through esterification of cellulose: a review of chemistry and application. *Cellul.* 25, 3703–3731. <https://doi.org/10.1007/s10570-018-1830-3>.
- Yuen, S.-N., Choi, S.-M., Phillips, D.L., et al., 2009. Raman and FTIR spectroscopic study of carboxymethylated non-starch polysaccharides. *Food Chem.* 114, 1091–1098. <https://doi.org/10.1016/j.foodchem.2008.10.053>.
- Zhang, K., Feng, W., Jin, C., 2020. Protocol efficiently measuring the swelling rate of hydrogels. *Methods x.* 7 <https://doi.org/10.1016/j.mex.2019.100779>.